Protein Science (1992), *1*, 1154–1161. Cambridge University Press. Printed in the USA.

Three-dimensional structure of the Fab fragment of a neutralizing antibody to human rhinovirus serotype 2

JOSÉ TORMO,[1] ELISABETH STADLER,[2] TIM SKERN,[2] HERBERT AUER,[2] OTTO KANZLER,[3] CHRISTIAN BETZEL,[4] DIETER BLAAS,[2] AND IGNASI FITA[1]

[1] Departament d'Enginyeria Química, Escola Tècnica Superior d'Enginyers Industrials, E-08028 Barcelona, Spain
[2] Institute of Biochemistry, University of Vienna, A-1090 Vienna, Austria
[3] Bender Vienna, Production Engineering and Biopilot Plant, A-1120 Vienna, Austria
[4] European Molecular Biology Laboratory (EMBL), c/o Deutsches Elektronen Synchrotron (DESY), D-2000 Hamburg 52, Germany

(RECEIVED February 11, 1992; REVISED MANUSCRIPT RECEIVED April 27, 1992)

Abstract

The crystal structure of the antigen-binding fragment of a monoclonal antibody (8F5) that neutralizes human rhinovirus serotype 2 has been determined by X-ray diffraction studies. Antibody 8F5, obtained by immunization with native HRV2 virions, cross-reacts with peptides of the viral capsid protein VP2, which contribute to the neutralizing immunogenic site B in this serotype. The structure was solved by the molecular replacement method and has been refined to an R-factor of 18.9% at 2.8 Å resolution. The elbow angle, relating the variable and constant modules of the molecule is 127°, representing the smallest elbow angle observed so far in an Fab fragment. Furthermore, the charged residues of the epitope can be well accommodated in the antigen-binding site. This is the first crystal structure reported for an antibody directed against an icosahedral virus.

Keywords: antibody; crystal structure; human rhinovirus; viral neutralization

Human rhinoviruses (HRVs), members of the picornavirus family, are small icosahedral RNA viruses and are the main causative agent of the common cold. The determination of the nucleotide sequences of the genomes of several representatives of this serologically varied genus (reviewed by Stanway, 1990) together with the solution of the three-dimensional structures of HRV14 and HRV1A by X-ray crystallography (Kinemage 4; Rossmann et al., 1985; Kim et al., 1989) have illuminated the regions of the capsid that can induce an immune response. Furthermore, surface areas of the viral capsid constituting binding sites for monoclonal antibodies have been identified by analyzing mutants escaping neutralization; such mutations are generally located in the loops connecting the eight-stranded β-barrels of the capsid proteins VP1, VP2, and VP3. They lie near the three vertices of the icosahedral asymmetric unit and flank the "canyon," which has been proposed to contain the recognition site for the cellular receptors (Rossmann et al., 1985).

Reprint requests to: Ignasi Fita Rodriguez, Departament d'Enginyeria Química, Escola Tècnica Superior d'Enginyers Industrials, E-08028 Barcelona, Spain.

These data define four neutralizing immunogenic sites (NIm-Ia, Ib, II, and III) for HRV14 (Sherry et al., 1986), and three (designated A, B, and C) for HRV2 (Appleyard et al., 1990). Site A and B correspond to NIm-IA and NIm-II; however, whereas in HRV14 VP2 contributes most of the amino acid residues to NIm-II, in HRV2 VP1 is primarily involved in the architecture of site B. Site C does not correspond to any antigenic site in HRV14; it is constituted mostly of amino acids from VP2 and lies at a similar position as NIm-III in HRV14. As the three-dimensional structure of HRV2 has not yet been determined, the exact conformation and localization of the sites remains uncertain.

In contrast, little is known of the three-dimensional structure of antibodies neutralizing picornaviruses and of the antibody interactions at the molecular level. One such antibody (8F5), raised against native virions, was found to bind not only to the viral particle in its native conformation, but also to the viral protein VP2 on Western blots. This property was used to define the region of the binding site by bacterial expression of various deletion mutants of VP2; the binding site lies between residues 153 and 164 (Skern et al., 1987). This polypeptide segment is

located in the region of site B and is analogous to the Nim-II antigenic site on HRV14, which appears as a "puff" on the viral particle surface between strands βE and βF of the eight-stranded β-barrel (Kinemage 4; Rossmann et al., 1985). As the antibody 8F5 also recognizes a peptide bearing this sequence, an extensive analysis of the recognition site was carried out with a set of overlapping peptides. These experiments defined the minimal binding site as the sequence TRLNPD, covering residues 160–165 of VP2. Furthermore, a peptide including this minimal binding site of 8F5 (residues 156–170) was used to raise peptide-specific antisera that both bind to and neutralize HRV2 (Francis et al., 1987; Hastings et al., 1990). In order to investigate the nature of the interaction between the viral capsid and antibody 8F5, we initiated crystallographic studies of the Fab fragment of 8F5 (Tormo et al., 1990). The crystal structure solution and the preliminary refinement of the Fab fragment at 2.8 Å, together with the determination of the amino acid sequence of the variable regions of the heavy and light chains, are presented in this work.

Results and discussion

Molecular structure

The quality of the electron-density maps (Fig. 1) was such that most residues could be positioned with confidence. Only some highly solvent-exposed portions of the molecule present weak density. In particular, two short regions from both chains, containing the cysteine residues involved in the unique interchain disulfide bridge show very weak electron density; they are probably disordered. Thus, residues 134–138 of the heavy chain and the last residue of the light chain (Cys 220) have not been included in the current model (see Table 1 for the sequences). Side chains of residues 17, 32–33, 85, and 162–163 of the light chain and residues 28 and 191–192 of the heavy chain also showed poor density and high temperature factors. However, even for these residues the density corresponding to the main chain was clear. Residues Ser 32 and Arg 33 are placed in the middle of the L-CDR1 loop, the most prominent, very solvent-accessible complementarity-determining region (CDR) (Fig. 2; Kinemage 1). The most mobile residues, as derived from the temperature factors, appear to be from the light chain. In fact, the average temperature factors (Table 2) are significantly lower for the heavy chain, whereas there are no sharp differences between the constant and variable domains of the two chains. The heavy chain participates in many more intermolecular interactions; thus, crystal packing forces could restrain the flexibility of the heavy chain, lowering the corresponding temperature factors.

The global folding found for the 8F5 Fab fragment is consistent with all the crystallographically determined Fab structures (review by Amzel & Poljak, 1979; Alzary et al., 1988). The Fab 8F5 is nevertheless in a rather bent conformation, with the elbow angle between the constant and variable modules being only 127° (Fig. 2; Kinemage 1). This elbow angle, defined as the angle between the pseudodyad axes that relate the light chain and heavy chain domains in both the variable and constant modules, was found to vary from about 132° in New and McPC603 Fab fragments (review in Sheriff et al., 1988) to about 179° in the R19.9 and 36–71 Fab structures (Lascombe et al., 1989; Strong et al., 1991). The rotation–translation operations that optimize the superposition of the backbone atoms of the V_H and V_L domains are 173.59°, 1.5 Å; whereas for the C_L onto the C_H1 domains they are 169.54°, −1.47 Å.

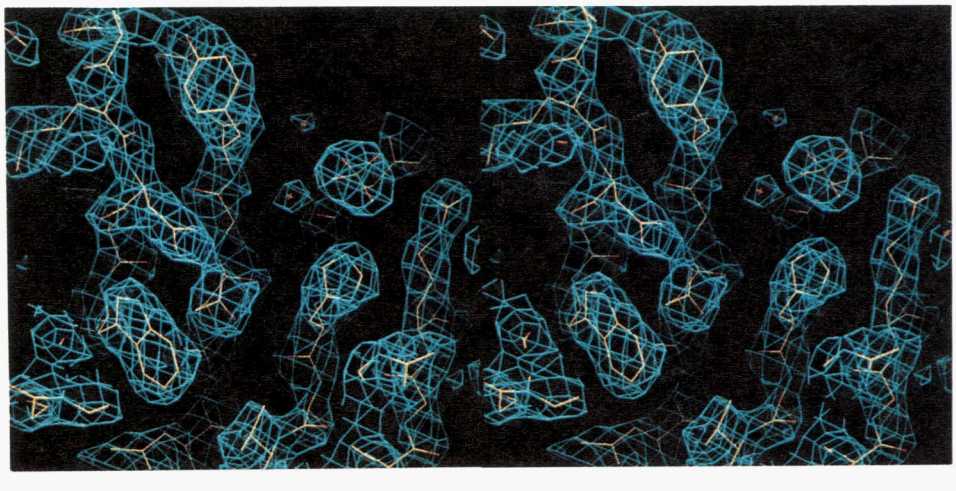

Fig. 1. Molecular model (represented with atom color code) and the electron-density map (in blue) calculated with coefficients (2Fo − Fc) in the H-CDR3 region. The quality of the map allows most side chains in the recognition pocket to be positioned with confidence. The sulfate ion and two nearby water molecules are visible in the upper right side of the photograph. As mentioned (see text), there are many aromatic residues around H-CDR3.

Table 1. *Nucleotide sequence and predicted amino acid sequence of the variable regions of the light and heavy chains of antibody 8F5*[a]

LIGHT CHAIN	HEAVY CHAIN
GACATTGTGATGACACAGTCTCCATCCTCCCTGACTGTGACAACGGGAGAGAAGGTCACT	GAGGT-CAGCTGCAGCAGTCCGG-GC-GAGCTTGTGAGGCCAGGGGCCTCAGTCAAATTG
AspIleValMetThrGlnSerProSerSerLeuThrValThrThrGlyGluLysValThr	GluValGlnLeuGlnGlnSerGlyAlaGluLeuValArgProGlyAlaSerValLysLeu
1 10 20	10 20
ATGACCTGCAAGTCCAGTCAGAGTCTGTTAAATAGTAGAACTCAAAAAAACTACTTGACC	TCCTGCACAACTTCTGGCTTCAACATTAAAGACATCTATATACACTGGGTGAAGCAGAGG
MetThrCysLysSerSerGlnSerLeuLeuAsnSerArgThrGlnLysAsnTyrLeuThr	SerCysThrThrSerGlyPheAsnIleLysAspIleTyrIleHisTrpValLysGlnArg
30 40	30 40
TGGTACCAGCAAAAACCAGGACAGTCTCCAAAATTGTTGATCTACTGGGCATCCACTAGG	CCTGAACAGGGCCTGGAGTGGATTGGAAGGCTTGATCCTGCGAATGGTTATACTAAATAT
TrpTyrGlnGlnLysProGlyGlnSerProLysLeuLeuIleTyrTrpAlaSerThrArg	ProGluGlnGlyLeuGluTrpIleGlyArgLeuAspProAlaAsnGlyTyrThrLysTyr
50 60	50 60
GAATCTGGGGTCCCTGATCGCTTCACAGGCAGTGGATCTGGAACAGATTTCACTCTCTCC	GACCCGAAGTTCCAGGGCAAGGCCACTATAACAGTAGACACATCCTCCAACACAGCCTAC
GluSerGlyValProAspArgPheThrGlySerGlySerGlyThrAspPheThrLeuSer	AspProLysPheGlnGlyLysAlaThrIleThrValAspThrSerSerAsnThrAlaTyr
70 80	70 80
ATCAGCGGTGTGCAGGCTGAAGACCTGGCAGTTTATTACTGTCAGAATAATTATAATTAT	CTGCACCTCAGCAGCCTGACATCTGAGGACACTGCCGTCTACTACTGTGATGGCTACTAC
IleSerGlyValGlnAlaGluAspLeuAlaValTyrTyrCysGlnAsnAsnTyrAsnTyr	LeuHisLeuSerSerLeuThrSerGluAspThrAlaValTyrTyrCysAspGlyTyrTyr
90 100	90 100
CCGCTCACGTTCGGTGCAGGGACCAAGCTGGAGCTGAAACGG	AGTTACTATGATATGGACTACTGGGGTCCAGGAACCTCAGTCACCGTCTCCTCA
ProLeuThrPheGlyAlaGlyThrLysLeuGluLeuLysArgAlaAspAlaAlaProThr	SerTyrTyrAspMetAspTyrTrpGlyProGlyThrSerValThrValSerSerAlaLys
110 114 120	110 118 120
ValSerIlePheProProSerSerGluGlnLeuThrSerGlyGlyAlaSerValValCys	ThrThrAlaProSerValTyrProLeuAlaProValCysGlyAspThrThrGlySerSer
130 140	130 140
PheLeuAsnAsnPheTyrProLysAspIleAsnValLysTrpLysIleAspGlySerGlu	ValThrLeuGlyCysLeuValLysGlyTyrPheProGluProValThrLeuThrTrpAsn
150 160	150 160
ArgGlnAsnGlyValLeuAsnSerTrpThrAspGlnAspSerLysAspSerThrTyrSer	SerGlySerLeuSerSerGlyValHisThrPheProAlaValLeuGlnSerAspLeuTyr
170 180	170 180
MetSerSerThrLeuThrLeuThrLysAspGluTyrGluArgHisAsnSerTyrThrCys	ThrLeuSerSerSerValThrValThrSerSerThrTrpProSerGlnSerIleThrCys
190 200	190 200
GluAlaThrHisLysThrSerThrSerProIleValLysSerPheAsnArgAsnGluCys	AsnValAlaHisProAlaSerSerThrLysValAspLysLysIleGluProArg
210 220	210 218

[a] Protein sequence numbers are sequential. The amino acid sequences of the constant regions of the light and heavy chains, taken from Altenburger et al. (1981) and Yamawaki-Kataoka et al. (1981), respectively, are also included for clarity. Residues in the complementary determinant regions (Kabat et al., 1987) are underlined.

The Fab molecules are packed in the crystal lattice by means of two different groups of interactions (Fig. 3). Molecules related by twofold screw axes of symmetry parallel to the **c** crystal axis are linearly arranged in a head-to-tail configuration. This gives rise to contacts between residues from the L-CDR2 and H-CDR3 with residues from the constant domain of the light chain. However, these interactions only involve the most external residues of these CDRs, the majority of the antigen-binding site remaining solvent exposed. In the second group, molecules related by twofold screw axes parallel to the crystal axis **a** interact extensively through the variable and constant domains of the heavy chain. A strand of the internal sheet from the variable domain is hydrogen-bonded to another strand of the external sheet of the constant domain resulting in an extended eight-stranded antiparallel β-sheet. Similar types of intermolecular interactions have already been observed for two L-chain dimers and an Fab fragment, but involving different pairs of domains. In the Mcg and Loc L-chain dimers, the three-stranded sheets of neighboring constant domains interact across a local twofold axis to form a six-stranded β-sheet structure (Ely et al., 1978; Chang et al., 1985). On the other hand, in the Fab NQ10/12.5 the intermolecu-

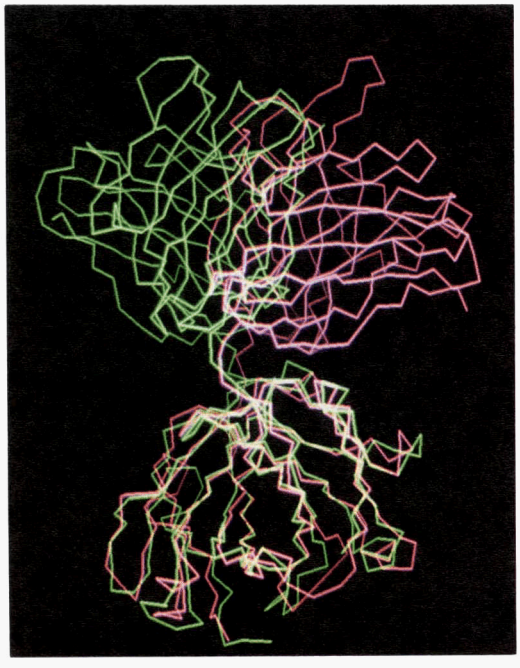

Fig. 2. The α-carbon skeleton of the Fab molecules, of R19.9 (in green) and 8F5 (in magenta), are represented simultaneously with overlapping constant modules. The differences in elbow angle values, 178 and 127, respectively, are reflected in the relative disposition of the variable modules. The most prominent loop, clearly visible in the CDR region of 8F5, corresponds to L-CDR1.

Table 2. *Crystallographic refinement data for Fab 8F5*[a]

Parameter	Standard deviation	Target value
Distance (Å)		
Bond length	0.022	0.02
Bond angle	0.053	0.03
Planar 1–4 distance	0.069	0.05
Planar groups	0.018	0.02
Chiral volume (Å^3)	0.225	0.15
Nonbonded contacts		
Single-torsion contacts	0.245	0.5
Multiple-torsion contacts	0.293	0.5
Possible hydrogen bonds	0.299	0.5
Torsion angle (°)		
Planar	3.1	3
Staggered	24.4	15
Orthonormal	18.5	20
	Light chain	Heavy chain
Average thermal factor		
Variable domain	31.62	22.53
Constant domain	32.62	25.77

[a] Measurements were based on 14,494 reflections with resolution limits of 7.0–2.8 Å.

lar β-sheet is formed between the internal sheets of two heavy chain variable domains related by the crystallographic twofold axis (Alzari et al., 1990).

The antigen-binding site

The main-chain conformation adopted by five of the six CDRs (Kinemage 2) conforms to some of the canonical structure models described by Chothia et al. (1989) on the basis of comparative studies of known Fab crystal structures. Thus L-CDR1 would correspond to the canonical form 3, L-CDR3 to the canonical form 1, H-CDR2 to the canonical form 2, and L-CDR2 and H-CDR1 to the only canonical forms proposed for them. H-CDR3, for which no canonical form was predicted due to its high conformational variability, forms in 8F5 a hairpin loop of the type 4:6 according to the β-hairpin nomenclature proposed by Sibanda and coworkers (1989) with the main-chain conformation in $\beta\alpha_R\alpha_R\gamma_R\,\alpha_L\beta$), respectively, for residues Tyr 100 to Met 105 (Kinemage 2). Although the conformation of the exposed loop of L-CDR1 corresponds to a canonical form as indicated above, it can also be described as another 4:6 β-hairpin with residue Gln 35 in the α_L conformation peculiar to this hairpin type.

The antigen-binding site of Fab 8F5 presents an irregular concave surface, the most prominent features being a shallow groove and the loop of L-CDR1 pointing to the solvent. The cavity or groove is located at the interface between the heavy and light chain variable domains. The floor of this cavity is formed by residues from L-CDR3, H-CDR1, H-CDR3, as well as several framework residues (Kinemage 3). Residues from the six CDRs and framework residues constitute the walls. Between them, aromatic residues, mainly Tyr, predominate and are partially accessible to the solvent. This situation is extreme for H-CDR3 with five tyrosines of a total of nine residues (Kinemage 2). The high frequency of aromatic amino acids, as observed in 8F5, is very often found in the ligand binding site of antibodies and histocompatibility glycoproteins (Bjorkman et al., 1987; Padlan, 1990; Mian et al., 1991).

The electron-density maps show a strong peak situated inside of the cavity of the antigen-binding site. The crystallization mixture contained two different ions that could account for this density; the high sulfate concentration (1.9 M) relative to that of phosphate (0.1 M) suggests the presence of a sulfate ion. This ion is in contact with a number of residues and water molecules with which it interacts through hydrogen bonds and salt bridges (Fig. 4; Kinemage 3). Interestingly, the epitope recognized by monoclonal antibody 8F5 contains two acidic residues that have been proved to be crucial for the binding. Asp 165 has been identified by studying the reactivity of 8F5 with a series of overlapping peptides covering this region of VP2, as one of the six residues that form the minimal binding site (TRLNPD). Furthermore, analysis of

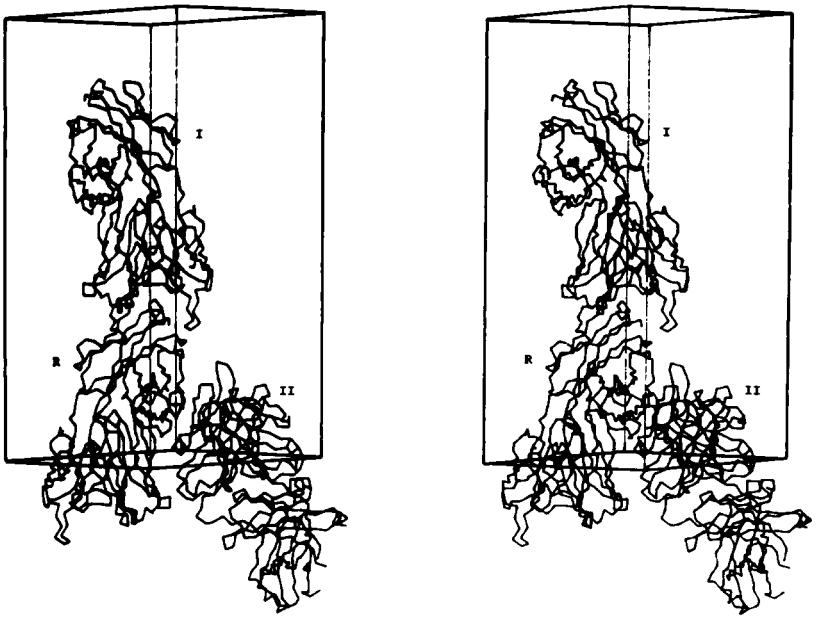

Fig. 3. Stereo drawing of the α-carbon skeleton of three 8F5 Fab molecules showing the two groups of intermolecular crystal contacts. The first type of contact (see text) gives a head-to-tail arrangement between the constant module of the Fab molecule closer to the unit cell origin (indicated as R in the figure) and the variable module of the symmetrically related Fab molecule (indicated as I). The second type of contact is formed between the heavy chain of the constant domain of the R molecule with the heavy chain of the variable domain of the symmetrical Fab molecule II.

neutralization-escape mutants have shown that the substitution of Glu 159, one of the residues flanking the minimal site, by Gly abolishes the binding of 8F5 to native virions. The sulfate-binding site could thus be occupied by the carboxylate group of Glu 159 or Asp 165 in complexes formed between either the peptide or the virion and the antibody.

A remarkable feature of the 8F5 recognition site is the presence of a pair of carboxylate groups, Asp 97 and Asp 106 of the heavy chain, at the bottom of the groove (Kinemage 3). These groups are not involved in any internal salt bridges, and in order to prevent repulsive electrostatic interactions, at least one of them must be protonated, even though the normal pK of the carboxylate group is about 4.4 and the crystallization solution was buffered at pH 6.0. The stored energy of this interaction might then be used as a specific mechanism to increase the strength of binding. Thus Arg 161 in the minimal binding site of VP2 could approach the two carboxylate groups in the antigen–Fab complexes.

In summary, the first crystal structure of an Fab fragment of an antibody neutralizing an icosahedral animal virus has been determined. The presence of the sulfate ion and the two interacting aspartate residues at the bottom of the antigen-binding pocket suggests that the binding to the antigen is heavily dependent on ionic interactions, which could provide the driving force for structural changes of the virion. The change of the isoelectric point of native virions as a consequence of the interaction with 8F5 favors this contention (unpubl.).

Materials and methods

Cloning of Fv regions and nucleotide sequencing

Cloning of the heavy and light chain variable regions was carried out as described (LeBoeuf et al., 1989) with the

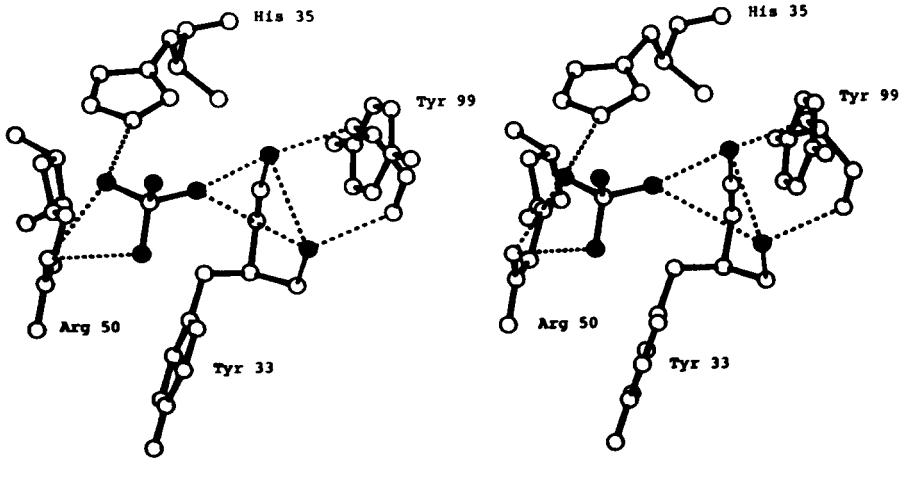

Fig. 4. Stereo drawing of the sulfate environment. The two water molecules and the sulfate oxygen atoms are represented as black filled circles. Possible hydrogen bonds are indicated with discontinuous lines. The four amino acid residues are from the variable domain of the heavy chain. The only oxygen from the sulfate not making any explicit hydrogen bond is fully accessible to the solvent and is pointing toward the entrance of the recognition pocket.

following modifications. DNA amplification was performed directly on the RNA–DNA hybrid in a Bio-Med thermocycler for 30 cycles set at 95 °C (1 min), 64 °C and 56 °C (1 min) for the heavy and light chain, respectively, and 72 °C (1.5 min). The amplified DNA was made blunt ended with T4 polymerase (Boehringer Mannheim), purified on an agarose gel, phosphorylated with polynucleotide kinase (Pharmacia), and ligated into SmaI-cleaved, dephosphorylated pUC8. To identify positive clones using the polymerase chain reaction (PCR), replicas were made from white colonies, bacteria were suspended in 30 μL 10× PCR buffer (Promega), incubated for 5 min at 95 °C, and insoluble material was pelleted in an Eppendorf centrifuge. Ten microliters of the supernatants was used for PCR reactions. Mini preps were made from positive colonies, and DNA was sequenced according to Sanger et al. (1977).

Preparation and crystallization of the Fab fragment

The preparation of murine monoclonal antibody 8F5 (IgG2a, κ), and the production, purification, and crystallization of its Fab fragment have been published (Skern et al., 1987; Tormo et al., 1990).

Crystallization was performed by vapor diffusion against 1.8 M ammonium sulfate, 0.1 M potassium phosphate, pH 6.0, at 22 °C, with an initial protein concentration of 10 mg/mL. The crystals are orthorhombic with space group $P2_12_12_1$ and unit cell parameters $a = 59.7$ Å, $b = 86.8$ Å, and $c = 128.0$ Å. There is one Fab molecule per asymmetric unit, and the estimated solvent content is around 61%.

Data collection

One data set was collected at the EMBL outstation using synchrotron radiation ($\lambda = 0.96$ Å, in the beam-line X11 of the DORIS storage ring at DESY, Hamburg) and the image plate detector system; 74.187 observations yielded 16,579 unique reflections to 2.8 Å resolution. Integration and reduction of the intensities were carried out using the MOSCO program system and the different frames were scaled together giving an overall merging R_{sym} of 0.07. The final data set to 2.8 Å resolution contained 93.5% of the expected number of reflections with Fo > 2.5σ (Table 3).

Table 3. *Data collection statistics*

Resolution range (Å)	R_{sym}[a]	Number of measured reflections with Fo > 2.5σ	Ratio of measured (Fo > 2.5σ) to possible reflections
99.0–5.36	0.054	2,395	0.929
5.36–4.25	0.067	2,325	0.953
4.25–3.71	0.075	2,300	0.948
3.71–3.37	0.087	2,296	0.961
3.37–3.13	0.107	2,271	0.945
3.13–2.95	0.150	2,221	0.931
2.95–2.80	0.196	2,086	0.879
Total	0.074	15,894	0.935

[a] $R_{sym} = \Sigma|I(h)i - \langle I(h)\rangle|/\Sigma\langle I(h)\rangle$.

Structure determination and refinement

The structure was determined by molecular replacement (Rossmann, 1972) using the program package MERLOT (Fitzgerald, 1988).

Antibody Fab fragments consist of two relatively rigid structural modules, the variable and the constant modules, connected by a flexible hinge or elbow formed by two short polypeptide links. This elbow angle had been seen to vary from 132° to 179° in known Fab structures (Sheriff et al., 1988; Lascombe et al., 1989; Strong et al., 1991). Because changes in the relative orientation of these two modules greatly influence the Patterson function, we have calculated independently the rotation and translation functions for each module following the example of Cygler and Anderson (1988a,b) for the structure solution of HED10 (Cygler et al., 1987).

The molecular models that proved useful in the analysis were the Fv module (V_L:V_H domains) of antibody R19.9 (Lascombe et al., 1989) (PDB file 1F19), and the constant module, C_L:C_H1 domains, of 17/9 (Rini et al., 1992). The fast rotation function (Crowther, 1972) was used with 10.0–4.0-Å resolution data and a radius of integration of 23.9 Å (Table 2).

The orientation and position of the Fv module were the first to be determined. In order to facilitate the interpretation of the results in the search for the orientation and translation of the constant module, one hybrid Fab molecule was constructed replacing the C_L:C_H1 domains of R19.9 for those of Fab 17/9 after superposition of their variable modules.

The rotation function of Lattman and Love (1970) was used to refine the positions of the peak of each probe. We successively used 2°, 1°, and 0.5° increments around the angle determined by the fast-rotation function. The Crowther–Blow (Crowther & Blow, 1967) translation function was then used with 10.0–4.0-Å resolution data, and the three Harker sections were examined.

The orientation and translation parameters were verified and further refined with BRUTE (Fujinaga & Read, 1987) using reflections between 5.0 and 4.0 Å. The model was then subjected to rigid body refinement with XPLOR (Brünger, 1990). At this stage, the Fv module of Fab R19.9 was replaced by the better refined Fv of Fab 17/9. During the final cycles the variable heavy, variable light, constant heavy, and constant light domains were allowed to move as four separate rigid bodies. The resulting R-

Table 4. *Orientation and rotation parameters for the molecular models*

Model	Peak order	Alpha	Beta	Gamma	rms[a]	First spurious peak rms	First spurious peak %
Rotation search: resolution 10.0–4.0 Å; radius 23.9 Å							
Vl:Vh R19.9	1	72.5	80	310	5.18	4.33	84
Cl:Ch1 17/9	2	102.5	86	160	4.54	4.58	100
		x	y	z			
Translation search: resolution 10.0–4.0 Å							
Vl:Vh R19.9							
Harker							
$x = 0.5$	3	–	17	14	3.55	4.32	100
$y = 0.5$	1	25	–	64	5.25	3.42	65.09
$z = 0.5$	13	76	67	–	3.05	3.46	100
Cl:Ch1 17/9							
Harker							
$x = 0.5$	2	–	14	10	3.57	3.75	100
$y = 0.5$	1	32	–	62	3.95	3.84	97.6
$z = 0.5$	1	83	65	–	4.03	3.45	85.6
		Initial	Two bodies	Four bodies			
R-factors for rigid body refinement							
Vl:Vh R19.9; Cl:Ch1 17/9		49.2	48.1	47.2			
Vl:Vh 17/9; Cl:Ch1 17/9		47.1	46.9	45.5			

[a] Root mean square deviations.

factor for data between 8.0 and 3.0 Å resolution was 45.5% (Table 4).

A (2Fo – Fc) electron density map was computed using 2,832 atoms remaining in the model after omitting the side chains of the noncommon residues between 17/9 and 8F5, residues from the six CDRs (13 from L-CDR1, 3 from L-CDR2, 6 from L-CDR3, 8 from H-CDR1, 3 from H-CDR2, and 6 from H-CDR3), and the residues of the switch region. The map was examined using the graphic program TOM/FRODO (Jones, 1985; Cambillau & Horjales, 1987) in an IRIS workstation 4D/706. Most of the truncated molecule was clearly visible in this difference map. After manual fitting of the residues to the density, the least-squares refinement procedure of Hendrickson-Konnert (Konnert & Hendrickson, 1980; Hendrickson, 1985) was started. The resolution was gradually increased during the refinement from 4.0 Å until the present limit of available data at 2.8 Å. Omitted residues or side chains were reintroduced in the model when visible on (2Fo – Fc) or (Fo – Fc) maps during the refinement process. One sulfate ion and three nearby water molecules have also been included to explain some prominent peaks of the electron-density map in the antigen-binding site. The final model obtained from the alternation of cycles of least-squares refinement and model building had an agreement R-factor of 18.9% for 14,827 reflections with Fo > 2.5σ in the resolution shell 7.0–2.8 Å (Table 2).

Acknowledgments

We thank Dr. I.A. Wilson and Dr. J. Rini for providing us with the coordinates of Fab 17/9, and Dr. S. Sheriff for sending us a UNIX version of the refinement programs. We also thank Dr. J.A. Subirana for his constant support. This work was funded by grants BT87-0009 and BIO 756/90 from the Comision Interministerial de Ciencia y Tecnología (Spain), the Österreichische Fonds zur Förderung der Wissenschaftlichen Forschung, and Boehringer Ingelheim. J. Tormo was a recipient of a fellowship from the Ministerio de Educación y Ciencia (Spain).

References

Altenburger, W., Neumaier, P.S., Steinmetz, M., & Zachau, H.G. (1981). DNA sequence of the constant gene region of the mouse immunoglobulin kappa chain. *Nucleic Acids Res. 9*, 971–981.

Alzari, P.M., Lascombe, M.B., & Poljak, R.J. (1988). Three-dimensional structure of antibodies. *Annu. Rev. Immunol. 6*, 555–580.

Alzari, P.M., Spinelli, S., Mariuzza, R.A., Boulot, G., Poljak, R.J., Jarvis, J.H., & Milstein, C. (1990). Three-dimensional structure determination of an anti-2-phenyloxazolone antibody: The role of somatic mutation and heavy/light chain pairing in the maturation of an immune response. *EMBO J. 9*, 3807–3814.

Amzel, L.M. & Poljak, R.J. (1979). Three-dimensional structure of immunoglobulins. *Annu. Rev. Biochem. 48*, 961–997.

Appleyard, G., Russel, S.M., Clarke, B.E., Speller, S.A., Trowbridge, M., & Vadolas, J. (1990). Neutralization epitopes of human rhinovirus type 2. *J. Gen. Virol. 71*, 1275–1282.

Bjorkman, P.J., Saper, M.A., Samraoui, B., Bennet, W.S., Strominger, J.L., & Wiley, D.C. (1987). Structure of a human class I histocompatibility antigen, HLA-A2. *Nature 329*, 506–512.

Brünger, A.T. (1990). *X-PLOR (Version 2.1) Manual.* The Howard Hughes Medical Institute and Department of Molecular Biophysics and Biochemistry, Yale University, New Haven, Connecticut.

Cambillau, C. & Horjales, E. (1987). TOM: A FRODO subpackage for protein-ligand fitting with interactive energy minimization. *J. Mol. Graphics 5*, 174–177.

Chang, C.-H., Short, M.T., Westholm, F.A., Stevens, F.J., Wang, B.-C., Furey, W., Solomon, A., & Schiffer, M. (1985). Novel arrangement of immunoglobulin variable domains: X-ray crystallographic analysis of the λ-chain dimer Bence-Jones protein Loc. *Biochemistry 24*, 4890–4897.

Chothia, C., Lesk, A.M., Tramontano, A., Levitt, M., Smith-Gill, S.J., Air, G., Sheriff, S., Padlan, E.A., Davies, D., Tulip, W.R., Colman, P.M., Spinelli, S., Alzari, P.M., & Poljak, R.J. (1989). Conformations of immunoglobulin hypervariable regions. *Nature 342*, 877–883.

Crowther, R.A. (1972). Fast rotation function. In *The Molecular Replacement Method* (Rossmann, M.G., Ed.), pp. 173–178. Gordon & Breach, New York.

Crowther, R.A. & Blow, D.M. (1967). A method of positioning a known molecule in an unknown crystal structure. *Acta Crystallogr. 23*, 544–548.

Cygler, M. & Anderson, W.F. (1988a). Application of the molecular replacement method to multidomain proteins. 1. Determination of the orientation of an immunoglobulin Fab fragment. *Acta Crystallogr. A44*, 38–45.

Cygler, M. & Anderson, W.F. (1988b). Application of the molecular replacement method to multidomain proteins. 2. Comparison of various methods for positioning an oriented fragment in the unit cell. *Acta Crystallogr. A44*, 300–308.

Cygler, M., Boodhoo, A., Lee, J.S., & Anderson, W.F. (1987). Crystallization and structure determination of an autoimmune anti-poly (dT) immunoglobulin Fab fragment at 3.0 Å resolution. *J. Biol. Chem. 262*, 643–648.

Ely, K.R., Firca, J.R., Williams, K.J., Abola, E.E., Fenton, J.M., Schiffer, M., Panagiotopoulos, N.C., & Edmunson, A.B. (1978). Crystal properties as indicators of conformational changes during ligand binding or interconversion of Mcg light chain isomers. *Biochemistry 17*, 158–167.

Fitzgerald, P.M.D. (1988). MERLOT, an integrated package of computer programs for the determination of crystal structures by molecular replacement. *J. Appl. Crystallogr. 21*, 273–278.

Francis, M.J., Hastings, G.Z., Sangar, D.V., Clark, R.P., Syred, A., Clarke, B.E., Rowlands, D.J., & Brown, F. (1987). A synthetic peptide which elicits neutralizing antibody against human rhinovirus type 2. *J. Gen. Virol. 68*, 2687–2691.

Fujinaga, M. & Read, R.J. (1987). Experiences with a new translation-function program. *J. Appl. Crystallogr. 20*, 517–521.

Hastings, G.Z., Speller, S.A., & Francis, M.J. (1990). Neutralizing antibodies to human rhinovirus produced in laboratory animals and humans that recognize a linear sequence from VP2. *J. Gen. Virol. 71*, 3055–3059.

Hendrickson, W.A. (1985). Stereochemically restrained refinement of macromolecular structures. *Methods Enzymol. 115*, 252–270.

Jones, T.A. (1985). Interactive computer graphics: FRODO. *Methods Enzymol. 115*, 157–171.

Kabat, E.A., Wu, T.T., Reid-Miller, M., Perry, H.M., & Gottesman, K., Eds. (1987). *Sequences of Proteins of Immunological Interest*, 4th Ed. National Institutes of Health, Bethesda, Maryland.

Kim, S., Smith, T.J., Chapman, M.S., Rossmann, M.G., Pevear, D.C., Dutko, F.J., Felock, P.J., Diana, G.D., & McKinlay, M.A. (1989). Crystal structure of human rhinovirus serotype 1A (HRV1A). *J. Mol. Biol. 210*, 91–111.

Konnert, J.H. & Hendrickson, W.A. (1980). A restrained-parameter thermal-factor refinement procedure. *Acta Crystallogr. A36*, 344–350.

Lascombe, M.B., Alzari, P.M., Boulot, G., Saludjian, P., Tougard, P., Berek, C., Haba, S., Rosen, E.M., Nisonoff, A., & Poljak, R.J. (1989). Three-dimensional structure of Fab R19.9, a monoclonal murine antibody specific for p-azobenzenearsonate group. *Proc. Natl. Acad. Sci. USA 86*, 607–611.

Lattman, E.E. & Love, W.E. (1970). A rotational search procedure for detecting a known molecule in a crystal. *Acta Crystallogr. B26*, 1854–1857.

LeBoeuf, R.D., Galin, F.S., Hollinger, S.K., Peiper, S.C., & Blalock, J.E. (1989). Cloning and sequencing of immunoglobulin variable-region genes using degenerate oligodeoxyribonucleotides and polymerase chain reaction. *Gene 82*, 371–377.

Mian, I.S., Bradwell, A.R., & Olson, A.J. (1991). Structure, function and properties of antibody binding sites. *J. Mol. Biol. 217*, 133–151.

Padlan, E.A. (1990). On the nature of antibody combining sites: Unusual structural features that may confer on these sites an enhanced capacity for binding ligands. *Proteins 7*, 112–124.

Rini, J.M., Schulze-Gahmen, U., & Wilson, I.A. (1992). Structural evidence for induced fit as a mechanism for antibody–antigen recognition. *Science 255*, 959–965.

Rossmann, M.G., Ed. (1972). *The Molecular Replacement Method.* Gordon & Breach, New York.

Rossmann, M.G., Arnold, E., Erickson, J.W., Frankenberger, E.A., Griffith, J.P., Hecht, H.J., Johnson, J.E., Kamer, G., Luo, M., Mosser, A.G., Rueckert, R.R., Sherry, B., & Vriend, G. (1985). Structure of a human common cold virus and functional relationship to other picornaviruses. *Nature 317*, 145–153.

Sanger, F., Nicklen, S., & Coulson, A.R. (1977). DNA sequencing with chain-terminating inhibitors. *Proc. Natl. Acad. Sci. USA 74*, 5463–5467.

Sheriff, S., Silverton, E., Padlan, E.A., Cohen, G., Smith-Gill, S., Finzel, B., & Davies, D.R. (1988). Antibody–antigen complexes: Three dimensional structure and conformational change. In *Structure and Expression* (Sarma, M. & Sarma, R.H., Eds.), Vol. 1, pp. 49–54. Adenine Press, New York.

Sherry, B., Mosser, A.G., Colonno, R.J., & Rueckert, R.R. (1986). Use of monoclonal antibodies to identify four neutralization immunogens on a common cold picornavirus, human rhinovirus 14. *J. Virol. 57*, 246–257.

Sibanda, B.L., Blundell, T.L., & Thornton, J.M. (1989). Conformation of β-hairpins in protein structures: A systematic classification with applications to modelling by homology, electron density fitting and protein engineering. *J. Mol. Biol. 206*, 759–777.

Skern, T., Neubauer, C., Frasel, L., Gründler, P., Sommergruber, W., Zorn, M., Kuechler, E., & Blaas, D. (1987). A neutralizing epitope on human rhinovirus type 2 includes amino acid residues between 153 and 164 of virus capsid protein VP2. *J. Gen. Virol. 68*, 315–323.

Stanway, G. (1990). Structure, function and evolution of picornaviruses. *J. Gen. Virol. 71*, 2483–2501.

Strong, R.K., Campbell, R., Rose, D.R., Petsko, G.A., Sharon, J., & Margolies, M.N. (1991). Three-dimensional structure of murine anti-p-azophenylarsonate Fab 36-71. 1. X-ray crystallography, site-directed mutagenesis, and modelling of the complex with hapten. *Biochemistry 30*, 3739–3748.

Tormo, J., Fita, I., Kanzler, O., & Blaas, D. (1990). Crystallization and preliminary X-ray diffraction studies of the Fab fragment of a neutralizing monoclonal antibody directed against human rhinovirus serotype 2. *J. Biol. Chem. 265*, 16799–16800.

Yamawaki-Kataoka, Y., Miyata, T., & Honjo, T. (1981). The complete nucleotide sequence of mouse immunoglobulin γ2a gene and evolution of heavy chain genes: Further evidence for intervening sequence-mediated domain transfer. *Nucleic Acids Res. 9*, 1365–1381.